HILO: Enabling Low-power, Dual-Band Communication using Tunnel Diode Oscillators

Dhairya Shah[§], Rajashekar Reddy Chinthalapani[§], Pramuka Sooriya Patabandige, Ambuj Varshney
National University of Singapore, Singapore
Email: {dhairya, rajashekar.c, pramuka}@u.nus.edu, ambujv@nus.edu.sg

***Abstract*—Wireless communication remains the most power-consuming operation in embedded systems. Low-power transmitters such as backscatter achieve microwatt-scale operation but produce weak signals susceptible to in-band interference and frequency-selective fading, particularly in non-line-of-sight settings. Multi-band transmission can mitigate these effects through spectral-domain redundancy rather than temporal-domain redundancy, improving reliability without sacrificing bitrate or latency. However, conventional multi-band radio transceivers require duplicated RF chains or power-hungry synthesizers. We introduce HILO, a tunnel diode-based frontend that enables dual-band operation from a single circuit. HILO inverts the conventional paradigm: rather than suppressing the harmonics inherent to tunnel diode nonlinearity, it harnesses them. An external device injection-locks the oscillator to a fundamental frequency, simultaneously stabilizing a higher harmonic and yielding two injection-locked carriers without a second oscillator or frequency multiplier. In transmit mode, HILO exploits self-oscillating mixing to modulate both carriers simultaneously; in receive mode, it uses autodyne downconversion at both frequencies. By turning an inherent nonlinearity into a feature, HILO achieves dual-band links while consuming under $210\,\mu\text{W}$.**

I. INTRODUCTION

Wireless communication is the most power-intensive operation in embedded systems. Despite sustained efforts in designing low-power transmitters, reducing energy consumption comes at the cost of link margin, making communication reliability a major challenge [1]–[3]. This is especially true for transmitters based on backscatter mechanisms [4] and tunnel diodes [5], [6], whose radiated signal strength is weaker than that of nearby active radio transmitters, making them susceptible to interference. The challenge is particularly severe in non-line-of-sight (NLoS) environments, where frequency-selective fading can create deep nulls, forcing conservative bitrates and retransmissions. For low-power communication, *reliability is a prerequisite for energy efficiency*.

Improving the reliability of weak-signal transmissions typically involves tradeoffs. Coding schemes sacrifice effective bitrate by adding payload redundancy [7]. Advanced post-processing such as machine learning increases receiver complexity and power consumption. HILO proposes a different approach: multi-band communication. By simultaneously transmitting and receiving replica information across multiple frequency bands, HILO introduces redundancy in the spectral domain rather than the temporal domain. This mitigates narrowband interference and reduces the probability that frequency-selective fading degrades all channels simultaneously. Because the bands operate in parallel, link reliability improves without incurring latency or bitrate penalties.

[§]Co-primary authors with equal contributions to this work.

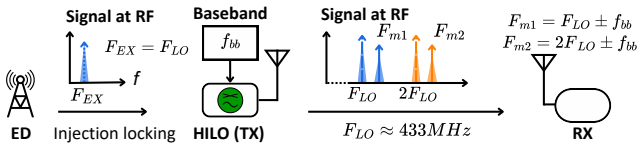

(a) HILO frontend as a transmitter

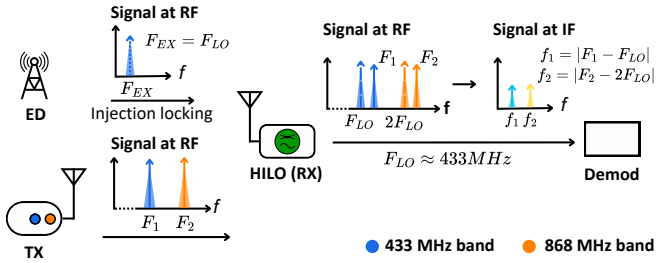

(b) HILO frontend as a receiver

Fig. 1. A carrier emitter device injection-locks the tunnel diode oscillator at $F_{\text{LO}} \approx 433$ MHz, which also generates a harmonic at $2F_{\text{LO}} \approx 868$ MHz. (a) HILO in transmit mode mixes a baseband f_{bb} signal, generating sidebands around the carrier and its harmonic for dual-band transmission. (b) HILO in receive mode is sensitive to signals near F_{LO} and $2F_{\text{LO}}$, using the autodyning property to downconvert signals in both bands.

Generating signals across multiple bands is incompatible with the power budget of typical embedded devices. Conventional transmitter architectures rely on phase-locked loops, frequency multipliers, and complex control logic; scaling these to support multiple bands increases energy overhead and circuit complexity. Recent backscatter systems [8]–[10] attempt to bypass this by exploiting tag nonlinearity to generate harmonics. However, these systems remain tethered to the delegation architecture, requiring a strong, proximate emitter device and suffering from the short transmission ranges intrinsic to conventional backscatter mechanism [6]. Furthermore, these prior efforts also focuses exclusively on the uplink. Real-world systems require bidirectional communication, a capability that existing multi-band low-power systems lack.

This paper introduces HILO, which stands for harmonic injection-locked oscillator, a low-power system that enables dual-band transmission and downconversion on a microwatt power budget. HILO achieves this by leveraging the inherent nonlinearity of tunnel diode. Recent tunnel diode oscillator (TDO) systems [5], [11] generate both a fundamental carrier and its harmonics, but treat the harmonics as unintended

and harmful emissions, employing filters and other techniques to suppress them. HILO inverts this paradigm. Instead of discarding these harmonics, we harness them. We demonstrate that naturally generated harmonics can be used to establish frequency diversity without increasing circuit complexity.

The tunnel diode is a highly nonlinear device. When coupled with a resonant LC tank, it generates not only a fundamental frequency but also harmonic content. Recent systems that stabilize TDOs without injection locking, such as AudioCast [12] and M^2 [13], show visible harmonics in their spectra. While SharpPeak [14] reports a harmonic-free spectrum, the cubic-like I-V characteristic of the tunnel diode makes harmonic generation unavoidable in principle. Measurement conditions strongly influence whether harmonics are observed. SharpPeak's spectra are captured over the air rather than via a conducted measurement at the oscillator terminals, so the reported suppression reflects the combined response of the TDO, matching network, antenna, and free-space propagation, all of which attenuate energy at $2F_{LO}$ more than at F_{LO}. Although conventional designs treat these harmonics as noise to be filtered, HILO exploits them to add spectral redundancy.

A free-running TDO is unstable and drifts with environmental changes [15]. HILO shows that injection-locking the fundamental simultaneously stabilizes the harmonics, yielding two frequency-locked carriers without a second oscillator or frequency multiplier. This allows the emitter device to operate at the lower frequency, benefiting from superior propagation while still stabilizing the high-frequency band.

HILO builds on recent work demonstrating the self-oscillating mixing (SoM) property of TDOs [5]. HILO shows that SoM modulates not only the fundamental but also the harmonic, enabling dual-band modulation without incurring any additional energy cost. Building on this propery, HILO modulates the carrier from TDO using frequency-shift keying (FSK) and demonstrate communication over tens of meters.

Finally, reception is essential for a complete communication system. Recent work demonstrates the ability of tunnel diodes to downconvert transmissions to intermediate frequency for receiver design [11]. HILO extends this capability, showing that harmonics generated by the TDO also enable downconversion via autodyning, paving the way for dual-band reception. Together, these contributions yield a dual-band tunnel-diode based transceiver frontend while consuming only $210\,\mu\mathrm{W}$.

II. Related Work

Harmonic backscatter. Recent work exploits the inherent nonlinearity in backscatter mechanisms. In RFID systems, a reader interrogates the tag with a fundamental tone, and the tag backscatters a response at a harmonic, typically the second [8]–[10]. This frequency separation mitigates the strong self-interference that plagues conventional backscatter links and improves robustness in cluttered environments [9]. Although harmonics were historically treated as parasitic, recent systems intentionally leverage harmonic backscatter for detection, localization, and sensing [10], [16], [17]. TagVibra [10] extracts phase from harmonic backscatter for sub-millimeter vibration sensing, Palazzi et al. [16] use amplitude-modulated harmonic backscatter for structural monitoring, and Piumwardane et al. [18] demonstrate high-resolution analog backscatter sensing. These systems are passive, using harmonics primarily for carrier self-interference isolation or sensing fidelity rather than to improve link reliability. Moreover, they inherit the limitations of backscatter: proximity to the emitter device and unidirectional communication (tag-to-reader only). HILO builds on these insights while addressing both limitations. It introduces a tunnel diode-based frontend that exploits TDO nonlinearity for dual-band operation and supports bidirectional communication through autodyning and SoM.

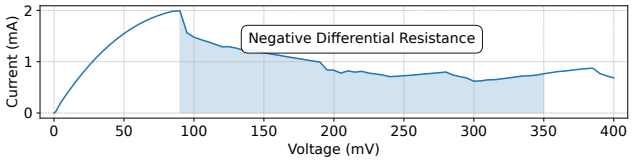

Fig. 2. I-V characteristics of GaAs 3I306E tunnel diode. The tunnel diode is biased in the negative differential resistance region and coupled with an LC resonant tank circuit to generate oscillations.

Tunnel diodes. They exhibit negative differential resistance (NDR) in their I-V characteristics, as shown in Figure 2. Because NDR occurs at very low voltages and currents, tunnel diodes are attractive for low-power RF designs. Previous work has exploited this property primarily for backscatter amplification. Amato et al. demonstrated up to $40\,\mathrm{dB}$ gain using tunnel diode-based reflection amplifiers in a $5\,\mathrm{GHz}$ backscatter tag [19], [20], while Adeyeye et al. designed a low-power repeater for RFID tags [21]. Eid et al. developed RFID tags that harvest energy from the carrier signal and use the tunnel diode for reflection amplification [22]. Amato et al. further proposed the harmonic tunneling tag, which biases a tunnel diode in its nonlinear region to achieve second-harmonic conversion gain over conventional passive harmonic backscatter [17]. HILO builds on these efforts but focuses on improving communication link reliability.

Recent efforts goes beyond backscatter, using tunnel diodes to build TDOs for transmitters [5], [12], [23] and receivers [11]. These achieve microwatt-level operation but sacrifice frequency stability. Varshney et al. address this instability through injection locking [5], while Thaddeus et al. exploit the frequency drift itself for vital-sign sensing [15]. The same nonlinearity that causes instability also generates strong harmonic components, as oscillations deviate from a pure sinusoid [24]. Previous designs suppress these harmonics for purity; HILO harnesses them to realize dual-band operation.

III. Design

HILO comprises three elements: a tag that generates carriers at both F_{LO} ($433\,\mathrm{MHz}$) and $2F_{LO}$ ($868\,\mathrm{MHz}$), an emitter device (ED) that injection-locks the tag at F_{LO}, and commodity receivers (e.g., TI CC1310) at one or both bands. In transmit mode, the TDO performs SoM with an input baseband signal, producing sidebands around both F_{LO} and $2F_{LO}$ for concurrent dual-band transmission. In receive mode, a conventional transmitter sends at either F_{LO} or $2F_{LO}$,

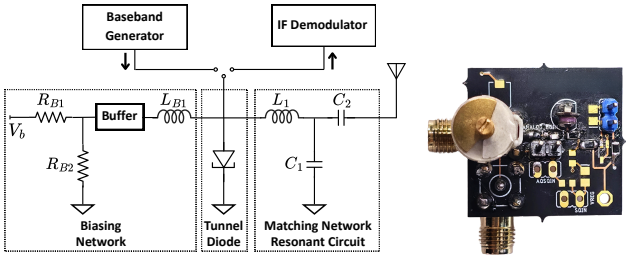

(a) Circuit Schematic (b) Prototype

Fig. 3. The HILO frontend consists of a tunnel diode coupled with an LC matching resonant tank, resulting in a TDO. Its nonlinear characteristics generate a fundamental carrier in the 433 MHz band along with its second harmonic in the 868 MHz band, enabling simultaneous dual-band operation.

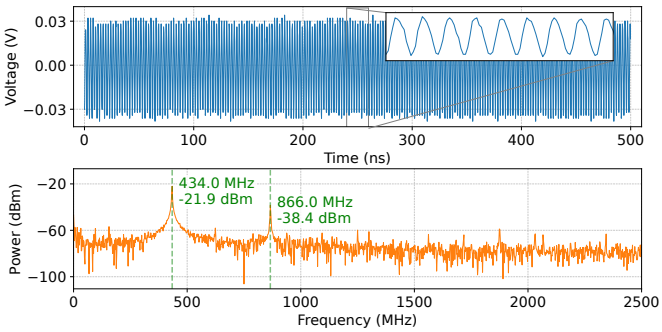

Fig. 4. TDO tuned near 433 MHz produces a harmonic in the 868 MHz frequency band, resulting in a dual-band carrier source using single component.

and the TDO downconverts the incoming signal to IF via autodyning for demodulation. When both bands are decodable, the receiver gains a frequency-diversity channel that improves link reliability. Figure 1 provides the system overview.

A. Dual-band Carrier Generation

HILO is designed using a TDO tuned to the 433 MHz ISM band by configuring the LC-tank circuit (Figure 3a). Because the tunnel diode is a strongly nonlinear device, its steady-state oscillation is not purely sinusoidal. The output spectrum contains a strong fundamental at F_{LO} and higher-order components at integer multiples kF_{LO}. In our design, the second harmonic at $2F_{LO}$ falls naturally within the 868 MHz ISM band, enabling dual-band carrier generation without an additional oscillator or mixing chain. We implement the HILO frontend with commercial off-the-shelf components on an FR-4 PCB (Figure 3b). The TDO uses a GE 3I306E tunnel diode [25]. Two SMA connectors couple directly to the tank circuit, allowing simultaneous connection of the ED and a spectrum analyzer during cabled characterization.

Figure 4 presents the time-domain representation of the output of the TDO and its corresponding spectrum. The spectrum is computed via an FFT (length $N = 2500$) of the waveform captured at 5 GSa/s using a Keysight DSOX3104T oscilloscope with 1 GHz bandwidth, connected via SMA cable with 50 Ω input termination. The resulting spectrum shows a fundamental tone near 434 MHz and a harmonic at 866 MHz, approximately 16 dB below the fundamental frequency.

Understanding nonlinearity and harmonics. The generation of the useful second harmonic arises from the distinct I–V characteristic of the tunnel diode. The current through

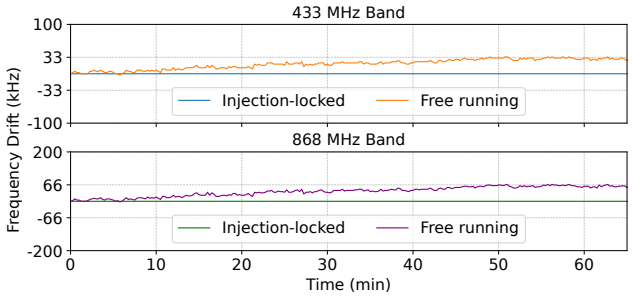

Fig. 5. Frequency stability analysis showing the drift of the fundamental and harmonic bands over time. Injection locking at F_{LO} stabilizes both the fundamental and the $2F_{LO}$ harmonic using a single ED reference.

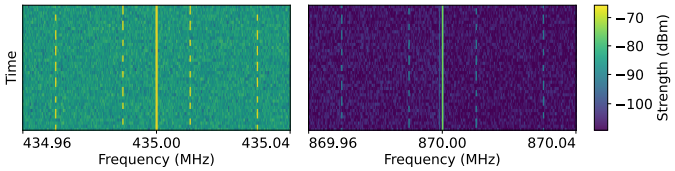

Fig. 6. The same baseband modulation applied once is translated to both 433 MHz and 868 MHz bands using a single HILO frontend.

the diode can be approximated by a polynomial expansion $i(v) = a_1 v + a_2 v^2 + a_3 v^3 + \dots$ around the bias point [24]. Higher-order terms in this expansion can also produce additional harmonic and intermodulation components; in this work, we focus on the dominant second-harmonic component that enables dual-band operation. When the tank circuit oscillates at the fundamental frequency $v(t) = A\cos(\omega_0 t)$, where $\omega_0 = 2\pi F_{LO}$, the quadratic term $a_2 v^2$ produces a component proportional to $\cos^2(\omega_0 t) = \frac{1}{2}(1 + \cos(2\omega_0 t))$. This $2\omega_0$ term is in the 868 MHz band. While typically considered parasitic interference and suppressed, HILO uses this component (−38.4 dBm) to serve as both the carrier for transmission and the effective local oscillator for downconversion.

Carrier frequency stability. A known challenge with TDOs is poor frequency stability [5], [11], [12], [15]. As shown in Figure 5, free-running TDOs drift significantly over time due to sensitivity to bias conditions and environmental perturbations such as temperature and antenna loading. While recent efforts [12], [13] have addressed this instability without external carriers, HILO stabilizes the TDO using an external carrier signal from an ED to injection-lock the oscillator. In injection locking, the TDO synchronizes its phase and frequency to the injected carrier. The harmonic component inherits this stability because it is generated from the locked fundamental. To quantify this, we apply a 433 MHz injection tone using a USRP SDR and monitor the output with a signal analyzer. As shown in Figure 5, injection locking at 433 MHz stabilizes both the fundamental and the 868 MHz harmonic, providing two frequency-locked carriers from a single ED.

B. Upconversion for Transmission

To enable transmission, HILO leverages the SoM property of the TDO [5]. The diode's nonlinear I–V characteristic multiplies the TDO voltage with the baseband signal, producing sidebands around both the fundamental and its harmonic.

Simultaneous upconversion. The HILO simultaneously upconverts the baseband signal to both the fundamental (F_{LO})

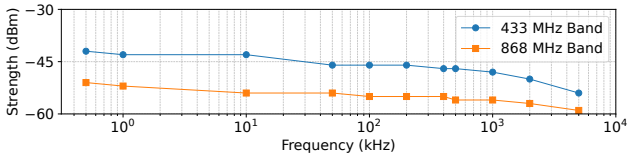

(a) Baseband frequency response

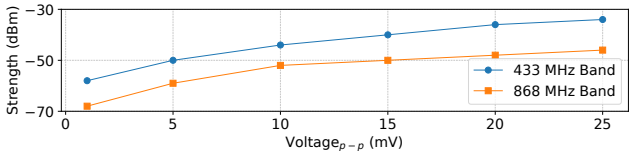

(b) Baseband amplitude response

Fig. 7. Characterization of mixed signal strength. (a) The mixing bandwidth extends beyond 1 MHz (b) The upconverted signal strength increases almost linearly with baseband amplitude.

and the harmonic ($2F_{LO}$). Unlike direct frequency modulation, where deviation scales with harmonic order, SoM acts as a mixer at both frequencies. The baseband frequency f_{bb} is preserved in the translation, producing sidebands at $F_{m1} = F_{LO} \pm f_{bb}$ and $F_{m2} = 2F_{LO} \pm f_{bb}$. We verify this experimentally by injecting a FSK baseband signal from an Analog Discovery 3 waveform generator at the HILO input port. The injection-locking signal is provided via a USRP in a cabled setup, and a spectrum analyzer captures the output. The resulting spectrum (Figure 6) confirms that the sideband offset from the carrier remains identical in both bands.

Characterizing upconversion. We characterize upconversion efficiency using the same cabled setup described previously, with a USRP providing the injection-locking signal and a spectrum analyzer capturing the output. An Analog Discovery 3 provides a sinusoidal baseband input, swept in frequency and amplitude. Figure 7a shows mixed signal strength against baseband frequency. The response remains relatively flat up to 1 MHz, confirming sufficient bandwidth to support higher data rates without significant attenuation. Figure 7b shows the linearity of the mixing process. As the peak-to-peak voltage of the baseband signal increases, sideband power increases nearly linearly. Consistent with the harmonic generation process, upconverted signal strength at 868 MHz is approximately 10 dB lower than at the fundamental but remains well above the sensitivity threshold of standard receivers.

C. Downconversion for Reception

Complementary to transmission, HILO functions as an autodyne mixer for reception. The diode's nonlinearity mixes incoming RF signals with the carrier to produce an intermediate frequency (IF) signal, which is demodulated.

Harmonic autodyning. HILO performs downconversion in two bands using a single device. In the 433 MHz band, incoming signals near F_{LO} mix with the fundamental to produce the IF signal. In the 868 MHz band, incoming signals near $2F_{LO}$ mix with the internally generated harmonic, which acts as an effective LO despite no dedicated 868 MHz oscillator present.

Sensitivity. It refers to the minimum signal strength that can be reliably detected and demodulated. We evaluate sensitivity

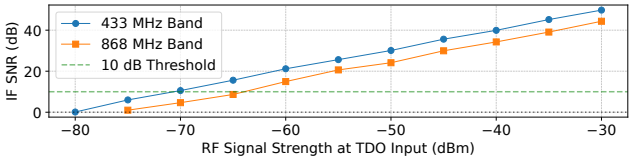

Fig. 8. Receiver sensitivity. Using a standard 10 dB SNR threshold, the system achieves a sensitivity of −70 dBm for the fundamental band and −62 dBm for the harmonic band.

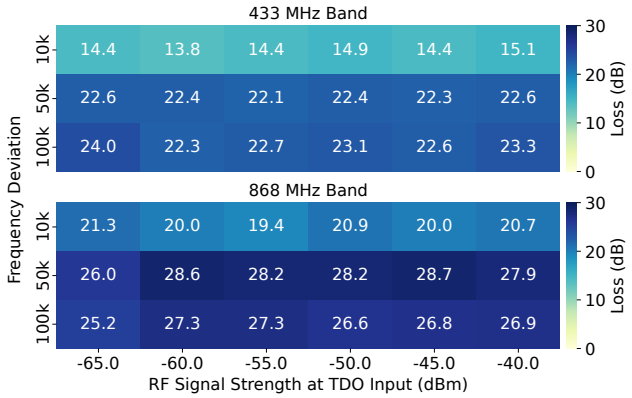

Fig. 9. Conversion loss. The 868 MHz harmonic band exhibits higher conversion loss (21 dB to 28 dB) compared to the fundamental band (15 dB to 23 dB) due to the weaker effective LO power at the frequency $2F_{LO}$.

using a cabled setup with two USRPs (one as the ED, the other as the transmitter), a Signal Hound BB60C spectrum analyzer, and a Mini-Circuits power combiner to interface with the HILO frontend. We vary the transmitter power and measure the strength of the downconverted signal, with the injection-locking signal at −40 dBm. The analyzer is configured with a resolution bandwidth (RBW) of 100 Hz and a span of 20 kHz to estimate the noise floor and calculate the signal-to-noise ratio (SNR). Figure 8 shows that the SNR of the downconverted signal increases with transmitter power.

For simple modulation schemes such as 2-FSK, an SNR of at least 10 dB is typically sufficient for low bit error rate (BER). Using this threshold, HILO can reliably receive signals down to −70 dBm in the fundamental band. Due to reduced conversion efficiency at the harmonic, the sensitivity threshold for the 868 MHz band is approximately −62 dBm.

Conversion efficiency. To characterize dual-band performance, we measure conversion loss, defined as the ratio of RF input power to IF output power. Figure 9 compares conversion loss for both bands across different input powers and frequency deviations, using the same cabled setup as the previous experiment. As expected, the 868 MHz band exhibits higher loss than the 433 MHz band, confirming that mixing with the weaker harmonic ($2F_{LO}$) is less efficient than mixing with the fundamental (F_{LO}). Despite reduced conversion efficiency at the harmonic, the system maintains a sensitivity of −62 dBm without requiring the power or complexity of a secondary active mixer.

IV. EVALUATION

Injection-locking range. To determine the practical operating range of the HILO frontend, we analyzed the maximum

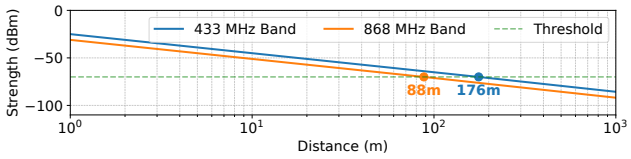

Fig. 10. Injection locking the HILO frontend at 433 MHz extends the effective range to 176 m, compared to only 88 m for TDO tuned to 868 MHz in an urban LoS deployment setting.

distance at which a ED can effectively injection-lock the tag. We observed that the locking threshold is $-70\,\mathrm{dBm}$ at the TDO input; below this power level, the oscillator phase noise dominates, and the lock is lost. Prior works have reported similar thresholds [5], [11]. We used the ITU-R P.1411 urban line-of-sight model [26] to simulate the propagation loss in a typical deployment environment. The ED is assumed to transmit with an EIRP of 10 dBm. Figure 10 compares the achievable locking range of a TDO tuned to a fundamental frequency of 433 MHz versus a TDO tuned to 868 MHz. The analysis demonstrates that at 433 MHz, the tag receives sufficient power ($\geq -70\,\mathrm{dBm}$) to maintain locking up to a distance of 176 m. In contrast, due to higher path loss at the higher frequency, an 868 MHz oscillator would only sustain a locking range of 88 m. This validates the HILO architecture: by utilizing a lower fundamental frequency for synchronization, we effectively double the injection-locking range compared to an oscillator at higher fundamental frequency.

Transmission range. We evaluate the transmission range of HILO by mixing the carriers generated by the TDO with a 2-FSK baseband waveform generated by an MSP430FR5969. The baseband is configured with a center frequency of 90 kHz, frequency deviation of 10 kHz, and data rate of 3 kbps. It follows a fixed packet structure consisting of a 4 B (byte) preamble, a 4 B synchronization word, a 1 B sequence number, a 1 B node identifier, and a 14 B payload. Cyclic redundancy check was disabled to enable analysis of corrupted packets. Experiments are conducted inside a university building in an indoor LoS setting with rich multipath due to walls and metallic structures. A USRP B200 located 10 m from the tag serves as the ED for injection locking. We use two TI CC1310 receivers to simultaneously receive the transmissions at the fundamental and harmonic bands while varying the receiver distance from 1 m to 30 m. We use Abracon 433 MHz to 960 MHz whip antennas having a gain of 3 dBi for the HILO transmitter, ED and receivers as shown in Figure 11a. Figure 11b shows the measured RSSI and BER averaged over 1000 packets across three trials. HILO maintains BER $\leq 10^{-2}$ up to 30 m in both bands. As expected, the 868 MHz link exhibits lower RSSI than 433 MHz due to the weaker harmonic component, but remains decodable. This also highlights the reliability of HILO to receive at the harmonic frequency, in case the fundamental undergoes frequency-selective fading. We did not evaluate beyond 30 m due to space constraints.

Power consumption. We measured the power consumption using the Keysight B2902A precision source/measure unit. The HILO frontend is biased at a supply voltage of 350 mV

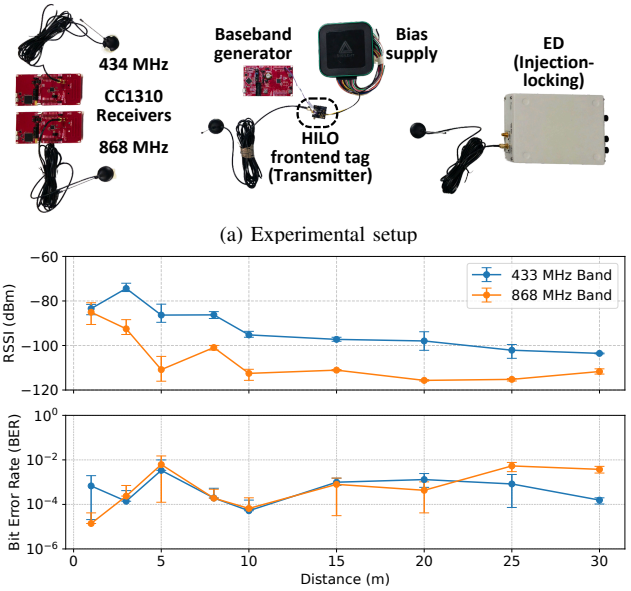

(a) Experimental setup

(b) Transmission range

Fig. 11. We conduct experiments in complex indoor line-of-sight environment to evaluate the transmission range. The harmonic link is consistently weaker yet remains decodable up to 30 m. The non-monotonic trends highlight frequency-selective fading and the two carriers can be impaired differently.

and draws a measured current of 0.6 mA, resulting in a static power consumption of 210 µW. The power budget of the complete system would additionally include the baseband generator for transmission (≈100 µW) and the demodulator pipeline for reception. Importantly, this 210 µW power budget supports simultaneous dual-band transmission or reception. Unlike conventional multi-band architectures that require a second RF chain to toggle between bands, HILO leverages the oscillator's inherent nonlinearities to generate the 868 MHz carrier alongside the 433 MHz fundamental without additional active circuitry. This effectively amortizes the energy cost across two frequency bands and enhances energy efficiency.

V. Discussion and Future Work

Interference mitigation. Figure 12 shows higher-order harmonics arising from the tunnel diode's nonlinearity. While the second harmonic ($2F_{LO}$) is intentionally exploited for communication, higher-order components (e.g., $3F_{LO}$ and $4F_{LO}$) appear approximately 25 dB and 35 dB below the fundamental. These constitute unintentional emissions that must be suppressed to meet regulatory spectral masks in commercial deployments. Our time-domain measurements in Figure 4 show that the oscilloscope's 1 GHz bandwidth naturally attenuates these components, suggesting that a simple low-pass filter or diplexer can provide sufficient suppression. A diplexer additionally enables separation of the fundamental and harmonic carriers, allowing band-optimized antennas for improved efficiency. We leave this as our future effort.

Supporting dual-band reception. While we demonstrate dual-band downconversion at both F_{LO} and $2F_{LO}$, this work does not implement a complete end-to-end receiver. A full receiver would additionally require analog baseband amplification and filtering, ADC sampling, and digital demodulation

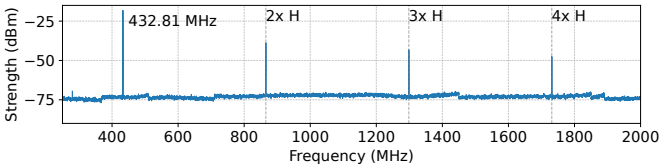

Fig. 12. Wideband spectrum of the TDO. While the second harmonic ($2F_{LO}$) is exploited for communication, higher-order components are present and require filtering for regulatory compliance.

to decode packets. To fully exploit frequency diversity, future systems could incorporate receive-side combining strategies (e.g., selection or maximal-ratio combining) that account for unequal SNR and band-specific impairments. Exploring these remains an important direction for future work.

Eliminating emitter-device. HILO currently relies on injection locking from an ED for TDO stability, thus partially retaining the delegation architecture common to low-power communication systems. Recent work has taken significant steps toward improving TDO stability and eliminating the need for an ED. AudioCast [12] combines a number of design choices, including purposefully operating at a lower frequency band, voltage filtering, and RF shielding, to stabilize the TDO at FM-band frequencies. A subsequent effort, SharpPeak [27], argues that controlled voltage transitions lead to improved TDO stability. However, all these systems rely on LC networks using discrete off-the-shelf components, which limits the Q-factor and results in long-term frequency instability beyond what commodity wireless standard requires, particularly under changing temperature and bias voltage conditions. Our recent work, M^2 [13], couples a tunnel diode with a high-Q SAW resonator, achieving orders of magnitude better stability than SharpPeak and AudioCast. M^2 also generates harmonics while retaining the SoM and autodyning properties, making it a promising foundation for designing standalone dual-band transceivers, which we leave as a future effort.

VI. CONCLUSION

We present HILO, a tunnel-diode-based RF frontend that enables dual-band operation using a single injection-locked oscillator. By locking the fundamental near $433\,\mathrm{MHz}$, HILO stabilizes and exploits its naturally generated second harmonic near $868\,\mathrm{MHz}$, eliminating the need for a second RF chain or frequency synthesis. A single baseband input is self-mixed onto both carriers for concurrent dual-band transmission, and the same frontend acts as an autodyne mixer to downconvert signals in both bands. This frequency-diverse operation improves robustness to frequency-selective fading and interference. Our prototype achieves reliable dual-band transmission beyond $30\,\mathrm{m}$ in LoS while consuming under $210\,\mu\mathrm{W}$ of power.

ACKNOWLEDGEMENTS

We thank the anonymous reviewers for their insightful comments. This work is funded by a Tier-1 grant from the Ministry of Education (A-8001661-00-00), a startup grant from ODPRT (A-8000277-00-00), and an unrestricted gift from Google through their Research Scholar Program (A-8002307-00-00-00), hosted at the National University of Singapore.

REFERENCES

[1] V. Liu *et al.*, "Ambient Backscatter: Wireless Communication out of Thin Air," in *ACM SIGCOMM 2013*.
[2] A. Varshney *et al.*, "LoRea: A Backscatter Architecture That Achieves a Long Communication Range," in *ACM SenSys 2017*.
[3] P. Nikitin *et al.*, "Theory and measurement of backscattering from RFID tags," *IEEE Antennas and Propagation Magazine*, 2006.
[4] J. Ensworth *et al.*, "Every smart phone is a backscatter reader: Modulated backscatter compatibility with bluetooth 4.0 low energy (BLE) devices," in *IEEE RFID 2015*.
[5] A. Varshney *et al.*, "Judo: addressing the energy asymmetry of wireless embedded systems through tunnel diode based wireless transmitters," in *ACM MobiSys 2022*.
[6] A. Varshney et al., "Tunnelscatter: Low power communication for sensor tags using tunnel diodes," in *ACM MobiCom 2019*.
[7] A. Varshney *et al.*, "Towards wide-area backscatter networks," in *ACM HotWireless 2017*.
[8] Z. Ye *et al.*, "Review on Recent Advances and Applications of Passive Harmonic RFID Systems," *IEEE JRFID*, 2023.
[9] Y. Ma *et al.*, "Harmonic-WISP: A passive broadband harmonic RFID platform," in *IEEE MTT-S IMS*, 2016.
[10] P. Li *et al.*, "RFID Harmonics-Based Sub-Millimeter Vibration Sensing," *ACM Transactions on Sensor Networks*, 2025.
[11] S. P. P. Medaranga *et al.*, "Unraveling the Missing Link in Low-power Communication: An Autodyning Receiver Architecture that Achieves a Long Range," in *ACM MobiSys*, 2025.
[12] R. R. Chinthalapani *et al.*, "AudioCast: Enabling Ubiquitous Connectivity for Embedded Systems through Audio-broadcasting Low-power Tags," *ACM IMWUT*, 2025.
[13] P. Sooriya Patabandige *et al.*, "Microwatt Microwave (M^2) Oscillator: Going Beyond the Delegation Architecture of Low-power Wireless Communication," in *ACM MobiSys 2026*, (To appear).
[14] M. Padmal, "Wireless communication systems for energy-constrained environments," Ph.D. dissertation, Uppsala University, Sweden, 2025.
[15] L. C. Q. Thaddeus *et al.*, "Tunnelsense: Low-power, non-contact sensing using tunnel diodes," in *IEEE RFID 2024*.
[16] V. Palazzi *et al.*, "Passive Wireless Vibration Sensors Based on the Amplitude Modulation of Harmonic Backscattering," *IEEE Transactions on Microwave Theory and Techniques*, 2024.
[17] F. Amato *et al.*, "The Harmonic Tunneling Tag: a Dual-Band Approach to Backscattering Communications," in *IEEE RFID-TA 2019*.
[18] D. Piumwardane *et al.*, "Unlocking the Potential of Low-Cost High-Resolution Sensing with Analog Backscatter," in *IEEE RFID 2024*.
[19] F. Amato et al., "Long range and low powered RFID tags with tunnel diode," in *IEEE RFID-TA 2015*.
[20] F. Amato, "Tunneling RFID tags for long-range and low-power microwave applications," *IEEE JRFID*, 2018.
[21] A. Adeyeye *et al.*, "5.8-GHz low-power tunnel-diode-based two-way repeater for non-line-of-sight interrogation of RFIDs and wireless sensor networks," *IEEE MWCL*, 2021.
[22] A. Eid *et al.*, "A 5.8 GHz Fully-Tunnel-Diodes-Based 20 µW, 88mV, and 48 dB-Gain Fully-Passive Backscattering RFID Tag," in *IEEE MTT-S IMS*, 2020.
[23] M. S. Mir *et al.*, "TunnelLiFi: Bringing LiFi to Commodity Internet of Things Devices," in *ACM HotMobile 2023*.
[24] G. Palumbo *et al.*, "Analysis and evaluation of harmonic distortion in the tunnel diode oscillator," in *IEEE ISCAS 2006*.
[25] N. Pulsar, *3I306E Gallium Arsenide Tunnel Diode Technical Specifications*, USSR Ministry of Electronic Industry, 2023. [Online]. Available: http://w140.com/tekwiki/wiki/Russian_tunnel_diodes
[26] ITU-R, "Recommendation ITU-R P.1411-13," International Telecommunication Union, Tech. Rep., 2025. [Online]. Available: https://www.itu.int/dms_pubrec/itu-r/rec/p/R-REC-P.1411-13-202509-I%21%21PDF-E.pdf
[27] M. Padmal *et al.*, "SharpPeak: Unlocking the True Potential of Tunnel Diodes for Low-Power Long-Range Communication," in *ACM SenSys 2026*.